

**GEOPHYSICAL CHARACTERIZATION OF THE UPEMBA GRABEN:
SEDIMENTARY THICKNESS ESTIMATION VIA SOURCE PARAMETER
IMAGING (SPI) OF REPROCESSED MAGNETIC DATA**

**Kenny Lose Manzembele ^{1*} , Bavon Diemu Tshiband ¹ , Dominique Westhondo
Osomba ², Patrick Vualu Ibula Mambenga ¹ , Michel Seya Kabongo ³ **

¹ Faculty of Petroleum, Gas and Renewable Energies, University of Kinshasa, D.R. Congo

² Faculty of Sciences and Technologies, University of Kinshasa, D.R. Congo

³ Faculty of Mines, Oil and Gas, Franco-American University, D.R. Congo

* Email (corresponding author): kenny.lose@unikin.ac.cd

DOI: 10.51865/JPGT.2026.01.02

ABSTRACT

The Upemba Rift, located in the southeastern Democratic Republic of Congo, constitutes a sedimentary sub-basin that remains largely underexplored despite its presumed petroleum potential. Covering an area of approximately 46,519 km², it recently attracted attention during the licensing rounds launched in 2022 by the Ministry of Hydrocarbons of the Democratic Republic of Congo. However, the absence of modern seismic data as well as detailed geological and geochemical surveys significantly constrains the assessment of its hydrocarbon prospectivity. The only available information derives from the magnetic survey conducted by CGG in 1986, which has already been interpreted in various studies.

Within this context, the present study – Geophysical characterization of structures in the Upemba Graben and estimation of sedimentary thickness using the Source Parameter Imaging (SPI) method: Reprocessing and integrated analysis of magnetic data – aims to propose a preliminary sedimentary model and to shed light on the morpho-tectonic evolution of the basin, thereby further highlighting its petroleum potential as well as the maximum sedimentary thicknesses of this intra-cratonic basin.

The results obtained are based on an integrated methodological framework combining a multimodel numerical approach, critical and comparative analysis, and an in-depth morpho-tectonic interpretation, together with sediment thicknesses derived from the SPI method, emphasizing their quantitative contribution. Taken together, these elements provide a robust preliminary argument that contributes to a better understanding of the morpho-tectonic history and sedimentary dynamics of the Upemba Graben and its petroleum system, thereby paving the way for increased interest from potential partners and renewed momentum in future exploration campaigns.

Keywords: geophysical characterization, Upemba Rift, lineaments, source parameter imaging (SPI) method, Kibara Group

INTRODUCTION

The Upemba Rift is among the sedimentary sub-basins of the Democratic Republic of Congo that exhibit petroleum potential yet to be formally assessed. It extends over an area of approximately 46,519 km² [1]. Although it attracted particular interest during the 2022 licensing rounds launched by the Ministry of Hydrocarbons of the DRC, the rift remains very poorly explored with respect to hydrocarbon exploitation. The identification of prospects – whether conventional or unconventional – has not yet been formally established, despite the presence of surface indications, notably within the Bukama territory located in the southeastern part of the rift. To date, the only available information on the formations consists of magnetic data acquired during the survey conducted by CGG in 1986 [1]. Since then, several studies have been undertaken, primarily focused on the re-evaluation and reinterpretation of these historical datasets, with the aim of estimating petroleum resources in most of the Congo basins to stimulate exploration and attract investors [2]. However, the work carried out in the Upemba Rift has not yet yielded results capable of significantly advancing our geological and petroleum understanding of this sector. From this perspective, our objective is limited to characterizing tectonic structures, reconstructing the morpho-tectonic history, and estimating the thickness of sedimentary formations by exploiting variations in magnetic susceptibility, while integrating geological constraints. Given the complexity of geological interactions within the Upemba Graben, this study is distinguished by its innovative character. It provides an updated synthesis of current knowledge regarding the reconstruction of the morpho-tectonic history of this sedimentary sub-basin and its sedimentary dynamics, particularly through thickness estimation. Furthermore, it sheds light on the petroleum potential of the graben through a multidisciplinary approach that enables the identification of prospective zones favorable to sediment accumulation.

GEOGRAPHICAL AND GEOLOGICAL SETTING OF THE STUDY AREA

The Upemba Graben, a tectonic depression located in the southeastern part of the Democratic Republic of Congo within Haut-Lomami Province, represents an intra-cratonic sedimentary basin bounded on both sides by border faults. It is characterized by rugged relief, punctuated by numerous lakes and multiple hydrothermal springs (Figure 1) [1], [3-13].

The regional geological context is dominated by the tectonic evolution of the Kibaran Belt, of Mesoproterozoic age (1,400–950 Ma), oriented along a northeast–southwest axis and extending for nearly 1,300 km [14], [10]. The configuration of geological structures observed in the region suggests a geotectonic dynamic of the subduction–collision type, which is considered to have led to the formation of the Upemba Rift, according to the works of [6], [9], and [14].

The Kibara Group, together with portions of the Katanga Group and the Ruzizi Group, forms the basement of the area [15]. Within this graben, a wide range of geological formations are present, including modern Holocene alluvium, Pleistocene and Pliocene deposits, Neogene, Paleogene, and Miocene units, Lower Cretaceous deposits formed during the most recent tectonic phase, as well as Lower Permian and Upper Carboniferous formations. In addition, lower Neoproterozoic sequences occur, including the conglomeratic complex [8], [16], [1]. However, to date, no evidence has been found for the existence of Triassic formations in the area [17], [1].

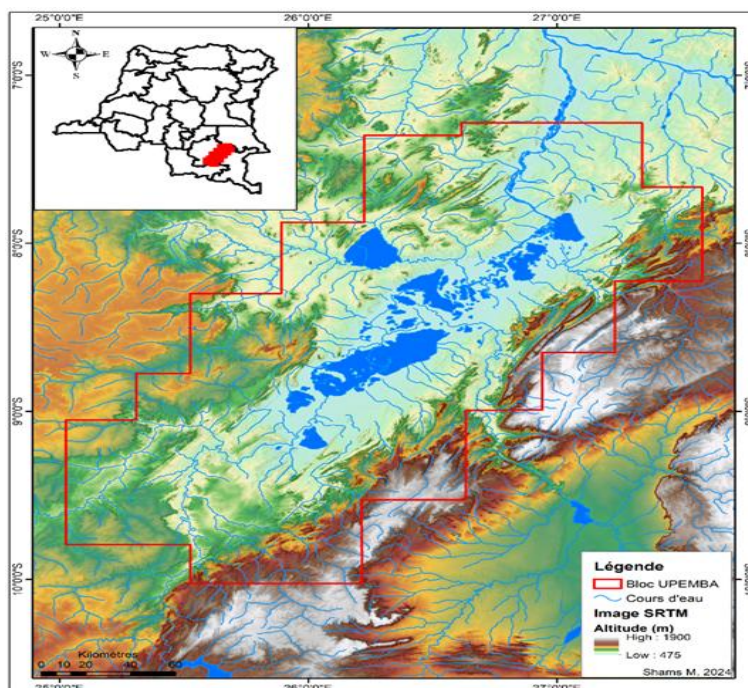


Figure 1. Topographic and hydrographic map of the Upemba Graben

MATERIALS AND METHODS

The materials and methods presented in this article provide a concise description of the different approaches employed as well as the software tools utilized. The objective of the adopted methodology is to facilitate data processing, analysis, and interpretation to better understand the geodynamic evolution of the studied sedimentary basin.

The methodology applied in this study is structured around two complementary components. The first consists of a critical documentary review, based on the examination of key reference works related to the geology of the Democratic Republic of Congo and to geophysics.

The second component of a numerical and multimodel nature, involves a combinatorial analysis integrating different magnetic and morphological models. This approach enabled the generation of several magnetic anomaly maps, which played a decisive role in constraining the sedimentary model of the study area. For this purpose, and with the aim of providing greater clarity regarding the methodological approaches employed in this study, we have synthesized in Table 1 the following elements: the complete set of magnetic filters applied, the key processing parameters, as well as the versions of the software packages utilized (Oasis Montaj, ArcGIS, RockWorks, Surfer).

The workflow can be summarized as follows: it began with the collection of data from the Ministry of Hydrocarbons of the Democratic Republic of Congo, followed by the application of various essential processing steps and corrections. These were carried out using software such as Geosoft Oasis Montaj 8.4, ArcGIS 10.8, and RockWorks 17, ensuring clarity and precision of the results and facilitating their interpretation. Figure 2 below illustrates the methodological framework of the multimodel numerical analysis.

Table 1. Geophysical data processing methods summarizing the main magnetic filters applied, the key processing parameters, and the software utilized.

Category	Method / Filter	Objectives	Key Processing Parameters	Data / Outputs	Software (version)
Transformations	RTP (Reduction to the Pole)	Center anomaly above the source (symmetric anomaly, more direct interpretation)	Magnetic field Inclination (I), Declination (D); IGRF field, 1985 model	Reduced-to-the-pole magnetic anomaly map	Oasis montaj 8.4
Convolution Filters	Low-pass	Smooth / remove high frequencies (noise, small irregularities)	Amplification of low frequencies	Regional anomaly map	Oasis montaj 8.4
Convolution Filters	High-pass	Highlight shallow structures / short wavelengths	Amplification of high frequencies	Residual anomaly map	Oasis montaj 8.4
Derivatives / Gradients	Gradient filter Dx ($\partial T / \partial x$)	Enhance boundaries/contacts in Y direction (sensitive to lineaments)	Horizontal derivative of magnetic field (dx); highlight N-S oriented lineaments	X-axis derivative map	Oasis montaj 8.4 / Surfer 27
Derivatives / Gradients	Gradient filter Dy ($\partial T / \partial y$)	Enhance boundaries/contacts in X direction	Horizontal derivative of magnetic field (dy); highlight E-W oriented lineaments	Y-axis derivative map	Oasis montaj 8.4 / Surfer 27
Derivatives / Gradients	Gradient filter Dz (1st vertical derivative $\partial T / \partial z$)	Strengthen shallow anomalies / contacts (very noise-sensitive)	Vertical derivative of magnetic field (dz); highlight shallow structures (generally in sedimentary cover)	Z-axis derivative map	Oasis montaj 8.4
Interpretation Attributes	Source Parameter Imaging (SPI)	Estimate depth / position of sources	Required derivatives (often 1st/2nd), SPI method, window/smoothing, thresholds (min amplitude / SNR), assumptions (2D contacts, etc.)	SPI depth map	Oasis montaj 8.4
Derivatives / Gradients	Total Horizontal Gradient (THG)	Highlight contacts/faults via horizontal gradients	$THG = \sqrt{Dx^2 + Dy^2}$; derivative method, smoothing, dx/dy, extraction thresholds (if picking)	THG grid	Oasis montaj 8.4 / Surfer 27
Structural Extraction	Lineaments (digitization / extraction)	Trace lineaments from THG, dx, dy, dz	Extraction criteria (manual/automatic), source layer (THG, dx, dy, dz)	Shapefile / polylines	ArcGIS 10.8
Structural Statistics	Lineament rose diagram	Analyze dominant directions (faults, fractures)	Lineament orientation (azimuth)	Rose diagram	RockWorks 17
Mapping / Layout	Cartographic layout & exports	Produce final maps (RTP, THG, AS, SPI, lineaments)	Symbology (palette, stretch), contours (interval), overlay transparency, graticule, scale, export (PDF/PNG, dpi)	Final maps	ArcGIS 10.8 / Surfer 27 / Oasis montaj 8.4

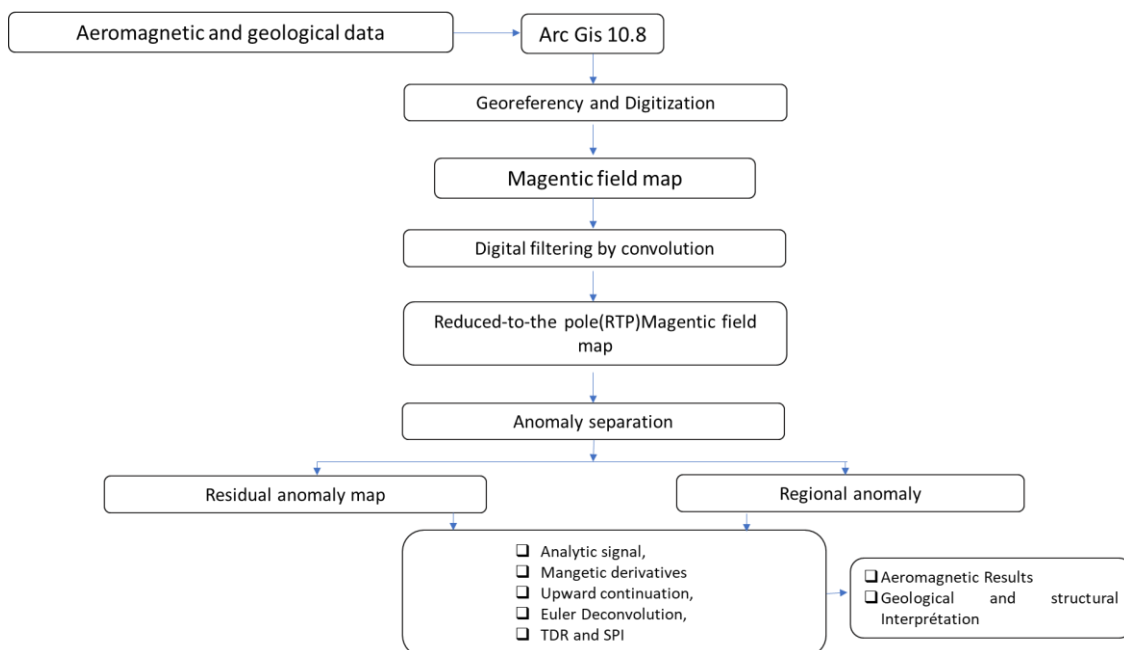


Figure 2. Workflow diagram illustrating the multimodel numerical analytical approach adopted in this study

RESULTS AND DISCUSSIONS

Based on magnetic data acquired during the CGG survey conducted in 1986, we obtained the magnetic anomaly map of the Upemba Graben, presented in Figure 3 below.

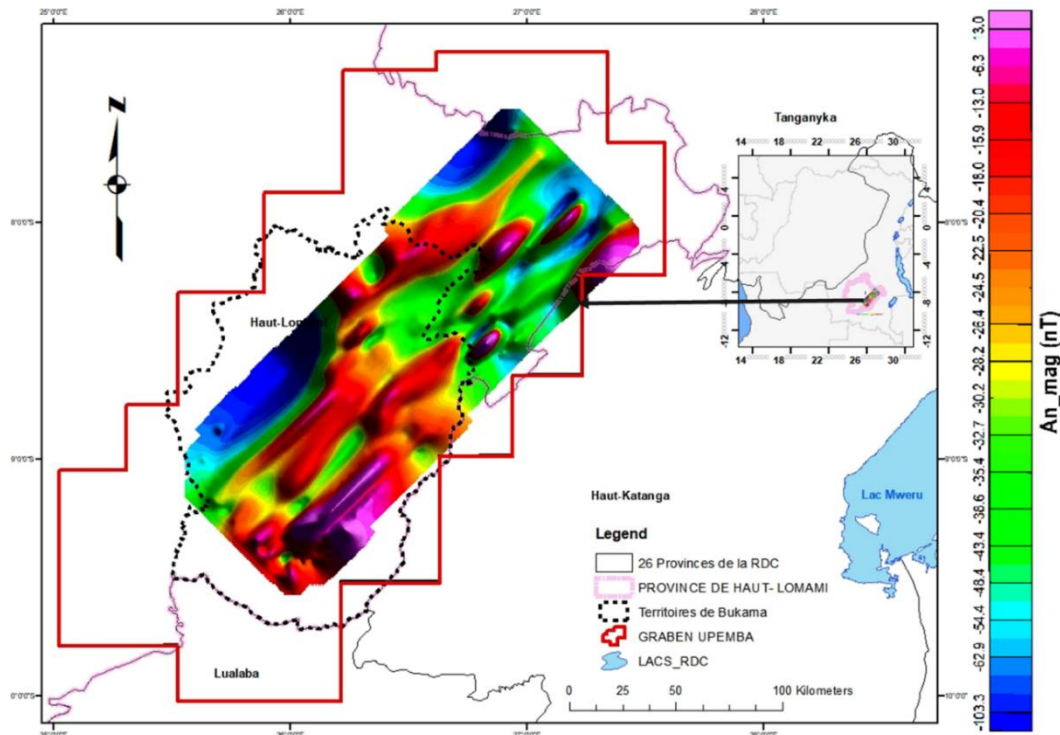


Figure 3. Magnetic anomaly map of the Upemba Graben, derived from raw magnetic data acquired during the geophysical survey conducted by CGG [18].

This enabled us to apply two numerical filtering methods: convolution and Euler deconvolution. The first filtering method is based primarily on three filters, the first of which is the reduction-to-the-pole of the magnetic anomaly field, presented in Figure 4.

It should be noted that reduction-to-the-pole is a filter that eliminates the distortion of anomalies caused by the inclination of the Earth's magnetic field [19], [20]. This filter thus repositions the magnetic and gravity anomalies directly above their geological source, using the Fourier transform [21].

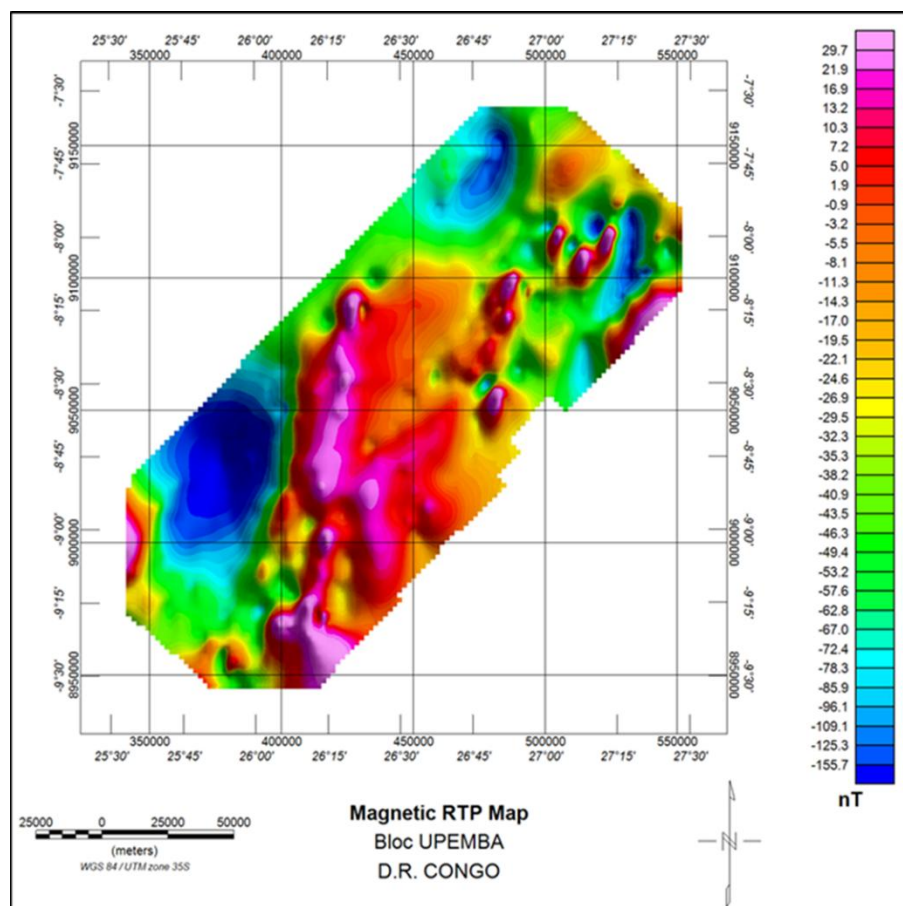


Figure 4. Magnetic anomaly map of the Upemba Graben, reduced to the magnetic pole, generated from reprocessed data of the geophysical survey conducted by CGG [18].

The processing applied yielded the reduced-to-the-pole magnetic anomaly map, thereby facilitating the separation of different anomalies. This procedure led to the development of iso-anomaly maps, derived from both regional and residual magnetic anomalies, presented in Figure 5 as color-shaded and relief-shaded images.

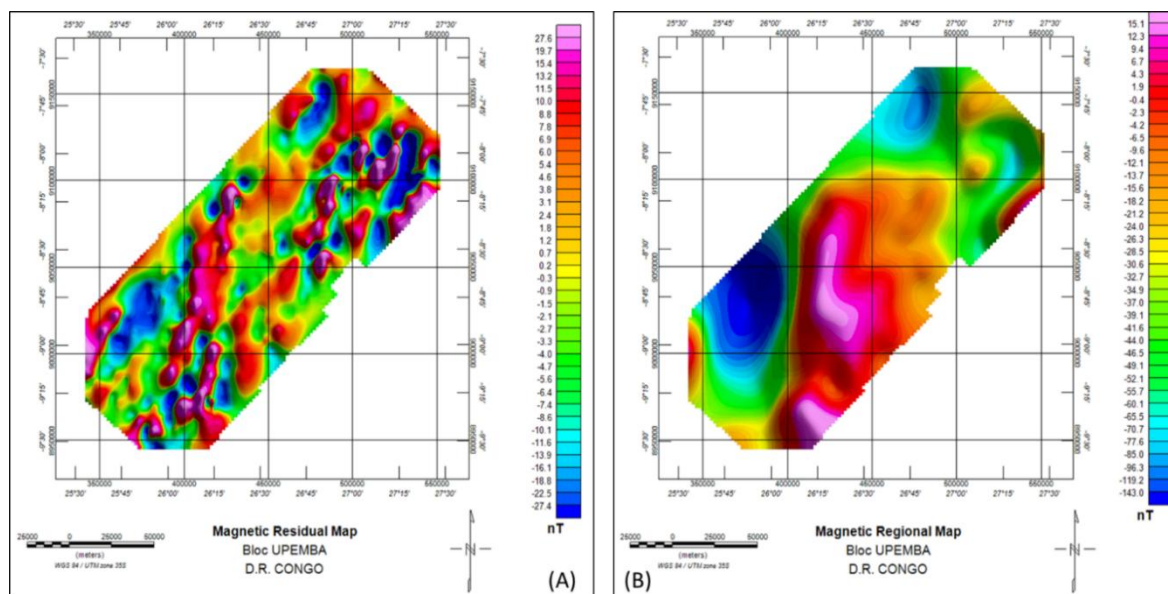


Figure 5. Residual magnetic anomaly map of the Upemba Graben (A), shown on the left, and regional magnetic anomaly map of the Upemba Graben (B), shown on the right, generated from reprocessed magnetic data acquired during the geophysical survey conducted by CGG [18].

We then applied a second filter, based on derivative analysis, using Geosoft Oasis Montaj 8.4 software. In the first step, the horizontal derivative [22] highlighted lithological contacts oriented north–south and east–west, corresponding respectively to the X and Y axes. These results are presented in Figure 6 below.

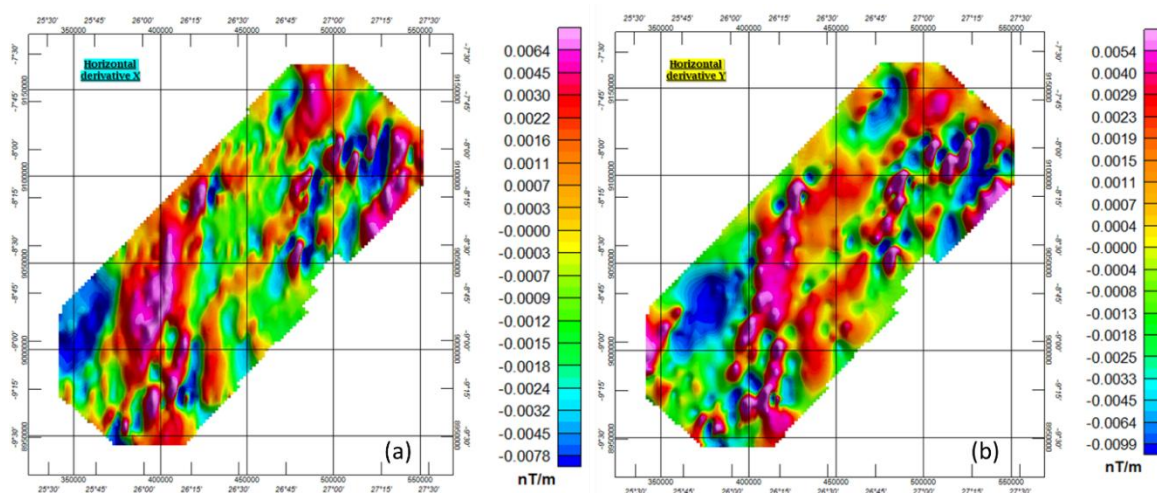


Figure 6. Magnetic anomaly maps of the Upemba Graben: (a) horizontal derivatives along the X -axis, shown on the left, and (b) horizontal derivatives along the Y -axis, shown on the right, generated from reprocessed magnetic data acquired during the geophysical survey conducted by CGG [18].

Subsequently, the application of the vertical derivative along the Z -axis, illustrated in Figure 7, enhanced the signatures of short wavelengths. This filter represents the rate of variation of the magnetic and gravity fields in the vertical direction. It is commonly applied to magnetic data to sharpen the edges of existing anomalies on the map [23].

It should be noted that the vertical derivative suppresses the long-wavelength components of the magnetic field and accentuates short-wavelength anomalies, thereby strengthening the amplitude of geological structures located near the surface. As a result, smaller anomalies become more readily apparent in areas of strong regional disturbances [23].

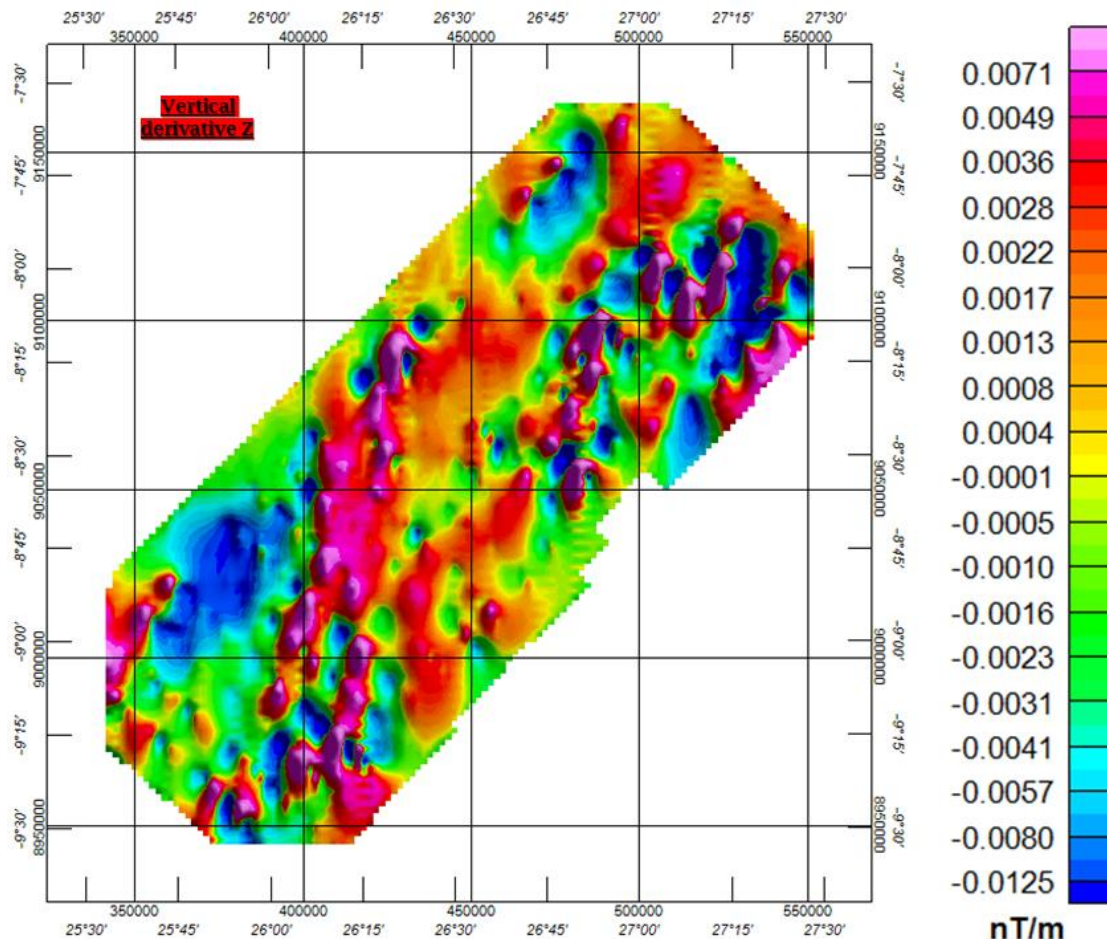


Figure 7. Magnetic anomaly map of the Upemba graben, vertically derived along the Z-axis, generated from reprocessed magnetic data acquired during the geophysical survey conducted by CGG [18].

By applying the upward-continuation filter and Euler deconvolution, we implemented the Tilt Angle Derivative (TDR) as well as the Total Horizontal Derivative (THDR) [22], [24]. The TDR and THDR were applied in such a way that weak and low-amplitude anomalies were enhanced relative to stronger anomalies.

This procedure facilitated the identification and isolation of structures of interest, thereby revealing fracture networks and deep structures [22], [24], [25]. It also enabled the mapping of lineaments and the extraction of their directional rose diagrams from aeromagnetic data, as shown in Figures 8 (a) and (b).

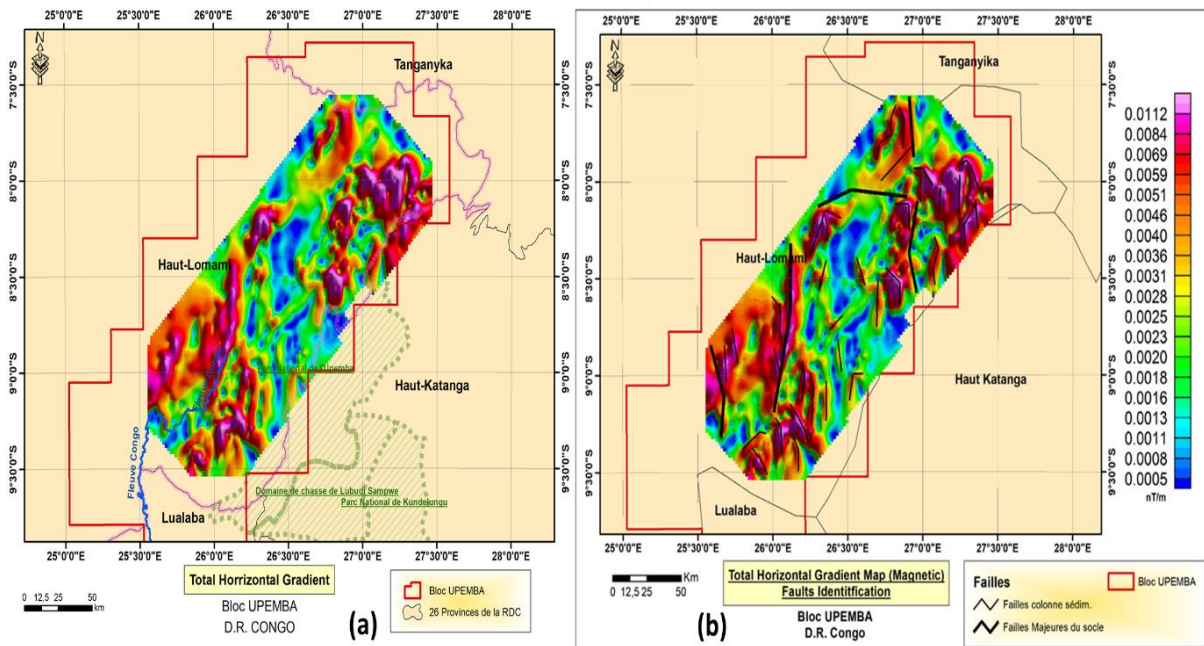


Figure 8. Total horizontal gradient magnetic anomaly maps of the Upemba Graben: (a) map shown on the left, and (b) map shown on the right, incorporating the identification of the main faults, generated from reprocessed magnetic data acquired during the geophysical survey conducted by CGG [18].

The trap structures indirectly detected in Figure 8 above were highlighted using the lineament map presented in Figure 9 below. It is important to note that the Tilt Derivative (TDR) is employed to enhance structural features and to detect the edges of the causative body in potential-field images, providing a qualitative indication of the dip of contacts associated with the TDR [26], [27], [28], [29], [30].

For this purpose, we used Surfer 25 software to import the generated grids and to trace the lineaments. In addition, ArcGIS 10.8 software allowed us to import shapefiles, format the lineaments, and calculate the coordinates of the line origins and endpoints.

These data facilitated the construction of directional rose diagrams of faults affecting both the basement and the sedimentary column, as illustrated in Figure 9, using RockWorks 17 software, based on the coordinates extracted from ArcGIS 10.8.

The examination of the Upemba Graben map (Figure 9) highlights four major structural orientations, corresponding to lineaments inherited from tectonic stresses that affected the crystalline basement during different geological phases:

- NW–SE (NE–SW stresses);
- N–S (E–W stresses);
- E–W (N–S stresses);
- N–S (E–W stresses, late phase).

These orientations indicate the successive influence of several major tectonic episodes: the Kibarian, Pan-African, Hercynian, and Alpine. The associated faults are expressed as normal faults, reverse faults, as well as dextral and sinistral strike-slip faults, reflecting the reactivation of pre-existing structures.

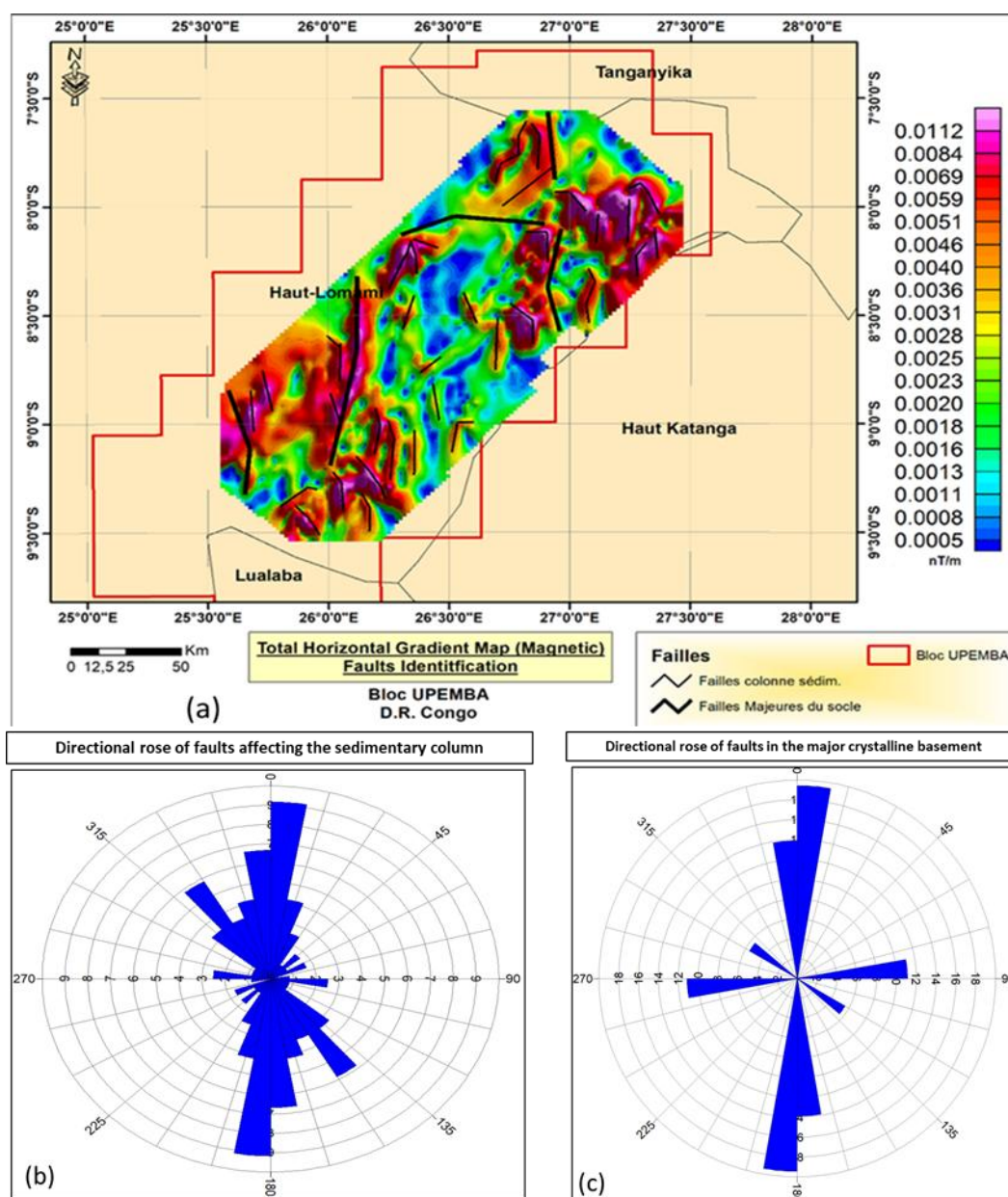


Figure 9. Total horizontal gradient magnetic anomaly map with identified faults (a), directional rose diagram of faults affecting the sedimentary column (b), and directional rose diagram of major faults (c), generated from reprocessed magnetic data of the Upemba Graben, acquired during the geophysical survey conducted by CGG [18].

The major faults illustrated in Figure 9(c) correspond to discontinuities within the crystalline basement, reactivated during each tectonic phase, sometimes in connection with subduction events. This leads us to formulate the following hypotheses regarding tectonic evolution:

1. Kibarian Phase (NE–SW)

The crystalline basement was affected by NE–SW oriented stresses, generating NW–SE lineaments.

2. Pan-African Phase (E–W compression)

This phase accentuated N–S lineaments, in relation to the major Congo River fault (S–N orientation), visible in Figure 8(a).

3. Hercynian Phase (Permo-Carboniferous)

N–S compressive stresses induced E–W lineaments. These faults operated as dextral and sinistral strike-slip structures, producing a pull-apart basin with tilted blocks. The regional presence of coal deposits bounded by faults (Figures 9(a, b, c) and 8(a, b)) supports this interpretation.

4. Alpine Phase (Late Cretaceous – Paleogene)

A second subsidence event, linked to E–W extensional stresses, generated N–S lineaments, resulting in the present-day configuration of the Upemba Graben.

In summary, four major tectonic phases have been identified, two of which produced significant subsidence events:

- The first during the Permo-Carboniferous (Hercynian tectonics);
- The second at the end of the Late Cretaceous – beginning of the Paleogene (Alpine tectonics).

The tectonic structures derived from the analysis of lineament maps (Figures 8 and 9) suggest rift-type architectures, probably associated with normal faults, horsts, and grabens with tilted blocks. These features are conducive to the formation of structural traps, while stratigraphic unconformities may generate stratigraphic traps, thereby offering significant petroleum potential. The regional magnetic anomaly results obtained from available datasets specifically from the CGG campaign conducted in 1986 [18] and presented in Figure 4 highlight three zones (north, northeast, and southwest) that reveal areas of deep subsidence, as shown in Figure 10, suggesting thick sedimentary basins.

The regional magnetic anomaly map presented in Figure 10 highlights three deep zones located in the north, northeast, and southwest. These areas of significant subsidence, with magnetic anomalies ranging from -65.5 to less than -143 nT, indicate substantial sedimentary thicknesses favorable to source-rock maturation and petroleum exploration, which can be associated with central basin or graben deposition.

Shallow zones, with anomaly values ranging from -40.5 to 17.1 nT, are revealed in the central part of the basin. These correspond to basement that is either exposed or near the surface, often associated with probable tectonic structures linked to horsts (uplifted blocks). Figure 11 illustrates the 2D and 3D maps, which emphasize both deep and shallow regional magnetic anomaly zones.

The sedimentary thickness of the subsidence zones identified below (see Figure 12) was estimated using the Source Parameter Imaging (SPI) method, a technique that applies an extension of the complex analytic signal to estimate magnetic depths. This technique, developed in [31], [32] and sometimes referred to as the local wavenumber method, is a profile- or grid-based approach for estimating the depth of magnetic sources. For certain source geometries, it accounts for contrasts between dip and susceptibility.

The method relies on the relationship between source depth and the local wavenumber (k) of the observed field, which can be calculated at any point in the data grid through horizontal and vertical gradients [31]. The depth is displayed in the form of an image. It is worth noting that

the local wavenumber map resembles a geological map more closely than a magnetic anomaly map, a susceptibility map, or their derivatives. Thus, after having previously identified the zones of major subsidence and applying the SPI method, we obtained the results presented in Figure 13. This figure illustrates a magnetic map generated using the SPI method, showing the basement depth beneath the sedimentary basin of the Upemba Block (DRC).

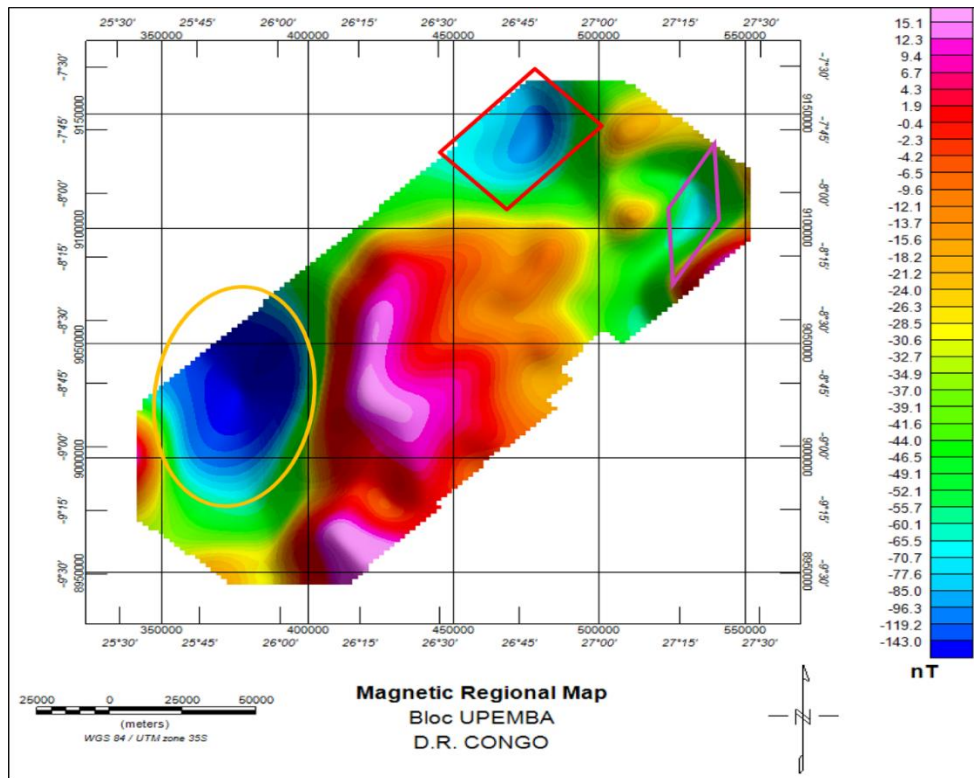


Figure 10. Regional magnetic anomaly map of the Upemba Graben, highlighting areas of deep subsidence, generated from reprocessed magnetic data acquired during the geophysical survey conducted by CGG [18].

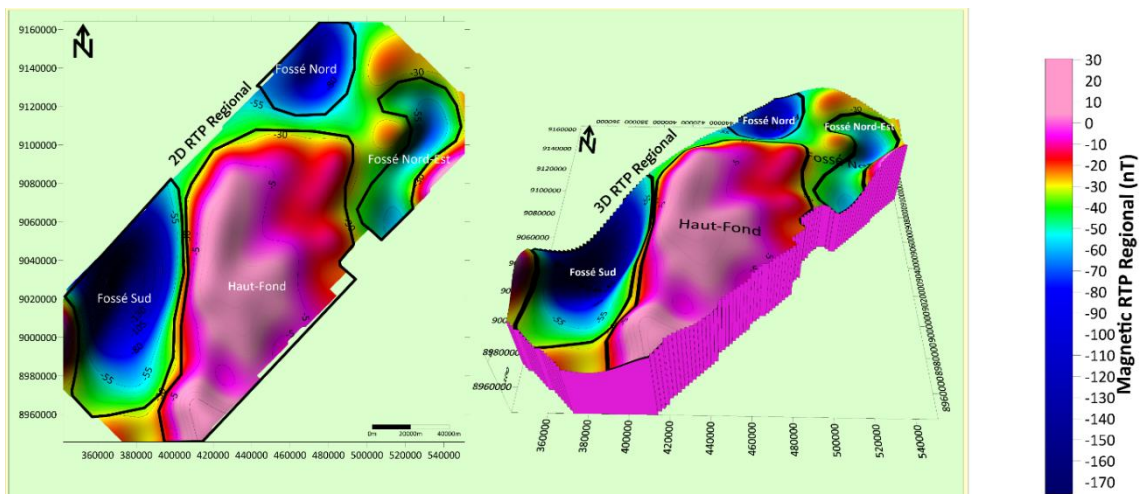


Figure 11. Regional magnetic anomaly maps of the Upemba Graben: (a) 2D representation on the left and (b) 3D representation on the right, generated from reprocessed magnetic data acquired during the geophysical survey conducted by CGG [18].

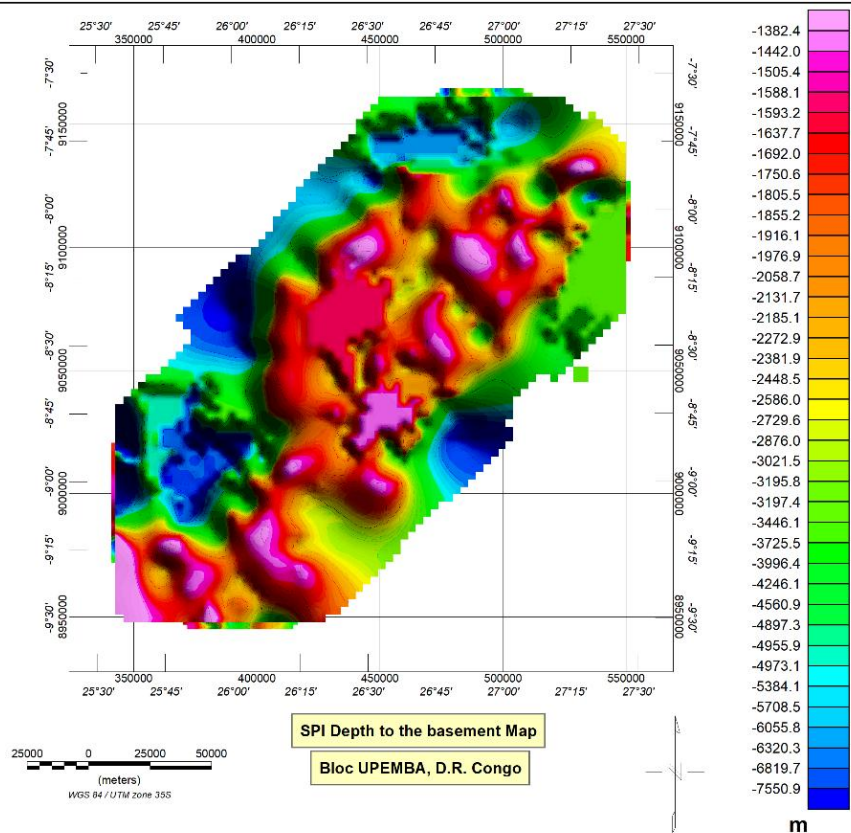


Figure 12. Basement depth map of the Upemba Graben (DRC), obtained using the SPI method, generated from reprocessed magnetic data acquired during the geophysical survey conducted by CGG [18].

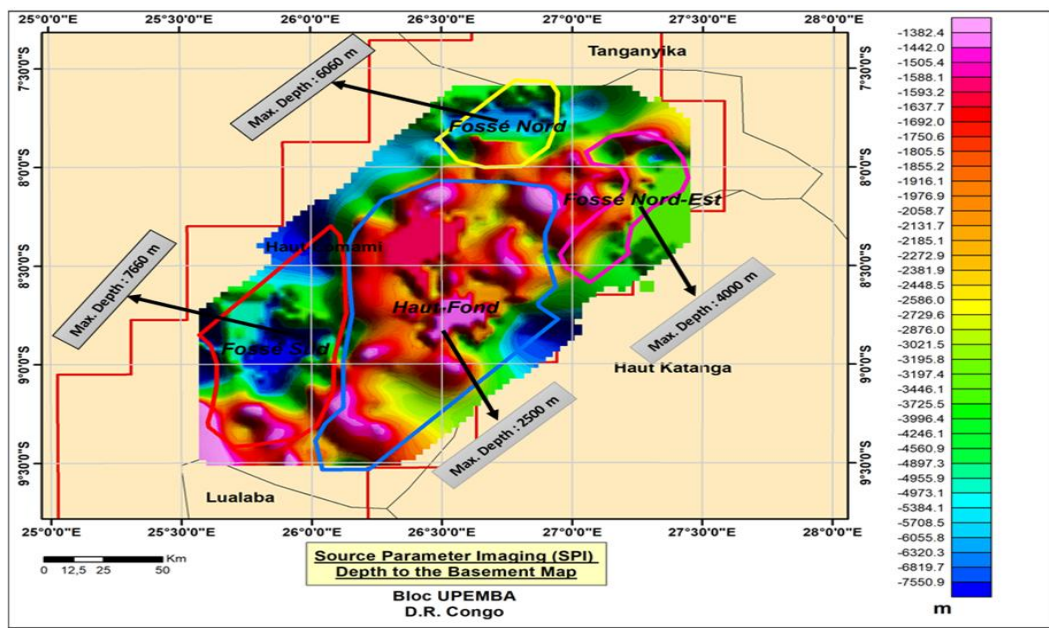


Figure 13. Magnetic anomaly map of the Upemba Graben used to estimate the depth of the crystalline basement by the SPI method, generated from reprocessed magnetic data acquired during the geophysical survey conducted by CGG [18]

The results obtained from the magnetic anomaly map of sedimentary thickness estimations indicate the maximum subsidence depths, with the greatest in the southwestern trough estimated at 7,660 meters, in the northern trough at 6,060 meters, and in the northeastern trough at 4,000 meters. These values correspond to zones of very thick sedimentary accumulation, as illustrated in Figure 14.

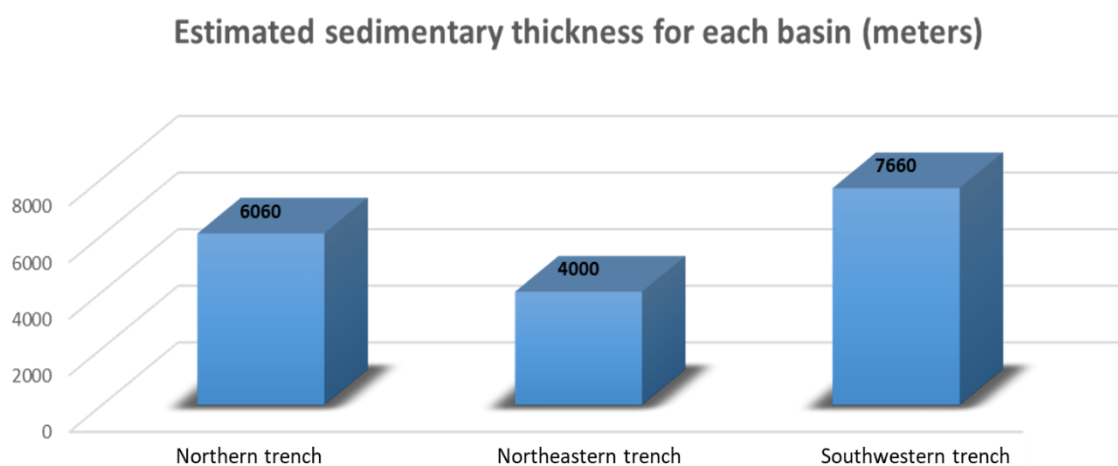


Figure 14. Histogram of estimated sediment thickness for the different troughs presented in Figure 13, derived from magnetic data acquired during the CGG survey conducted in 1986 [18].

In view of the foregoing, the three zones located to the north, northeast, and southeast emerge as areas of maximum subsidence, reflecting particularly active tectono-sedimentary dynamics within Upemba Graben, as illustrated in Figure 15. This figure provides a synthetic representation of the sedimentary model, including sediment thickness, the architecture of lineaments, as well as prospective zones derived from the reprocessed magnetic data of the Upemba Graben.

These geodynamic conditions are likely to promote source-rock maturation, thereby enhancing the processes of hydrocarbon generation and accumulation. Beyond their strictly petroleum interest, the identification of these zones contributes to a deeper understanding of regional geodynamic evolution, highlighting the mechanisms of differential subsidence and their role in basin structuring.

They thus represent strategic targets, not only for the valorization of energy potential but also for the development of more robust sedimentary and tectonic models. From this perspective, these sectors should be considered as priorities for the planning of future high-resolution seismic campaigns and exploratory drilling, with the aim of confirming their potential and refining petroleum development scenarios within Upemba Graben.

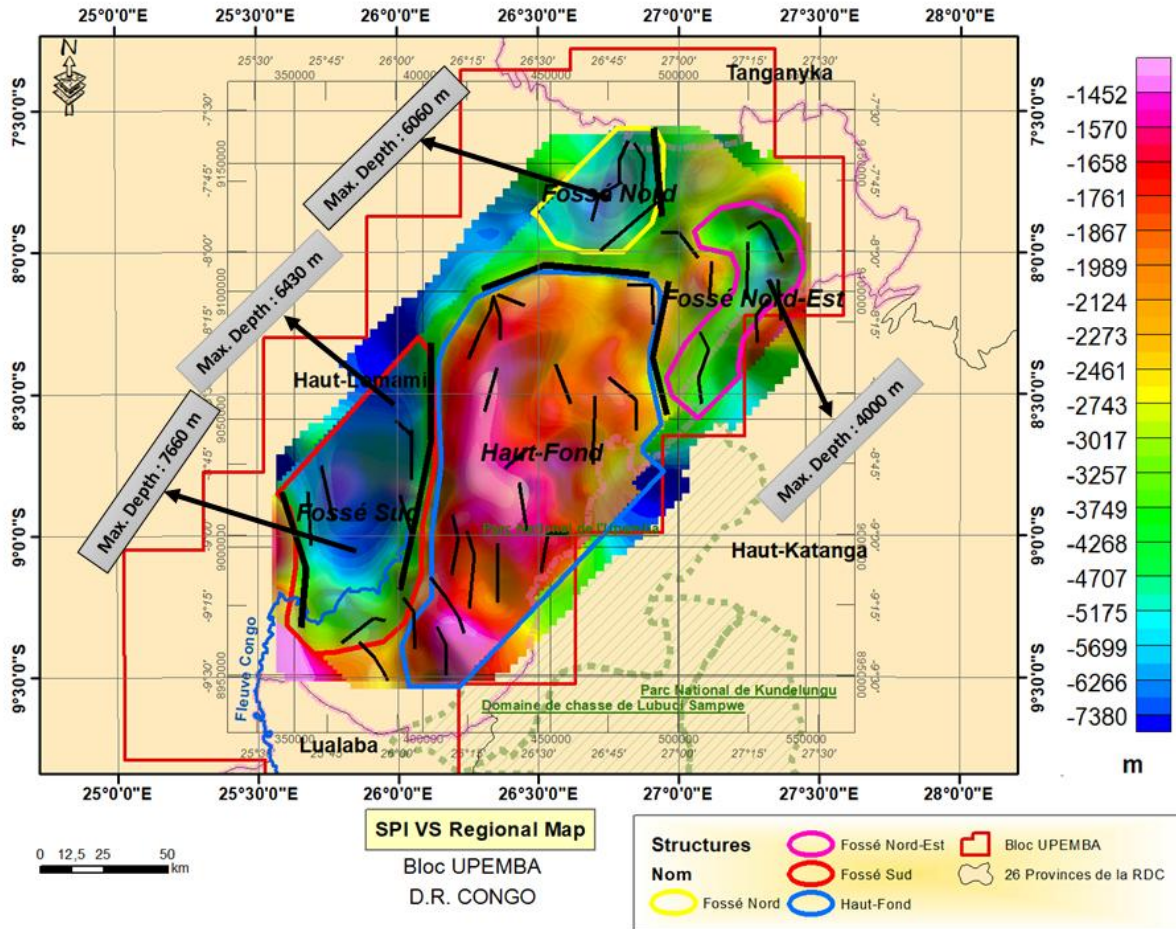


Figure 15. Synthetic map summarizing the sedimentary model, including deposit thickness, lineament architecture, and prospective zones derived from the reprocessed magnetic data of the Upemba Graben, generated from magnetic data acquired during the geophysical survey conducted by CGG [18].

CONCLUSIONS

The results highlight a structural consistency observed in Figures 8 and 9, expressed through faults whose northeast–southeast alignment follows a structural trend belonging to a broader geological framework extending both northward and southward. This structure is continuous with other lakes such as Albert, Edward, Kivu, and Moero, located along the western branch of the East African Rift. It indicates a common provenance and a tectonic emplacement process linked to crustal extension, characteristic of rift systems, as described in [5], [33].

The analysis of lineaments within the Upemba Graben reveals a tectonic system typical of rift settings, marked by normal faults, horsts, grabens, and tilted blocks. These structures provide a favorable framework for the development of structural traps, while the identified stratigraphic unconformities also suggest the potential presence of stratigraphic traps.

All of these features observed in the Upemba Graben fit into a geological history shaped by two distinct tectonic phases, each associated with a subsidence episode. The first phase, dated to the Permo-Carboniferous, is linked to Hercynian tectonics. The second phase likely occurred at the transition between the Late Cretaceous and the Early Paleogene, within the context of Alpine tectonics.

Three deep zones located in the northern, northeastern, and southwestern parts of the Upemba Graben are considered areas of significant subsidence and high prospectivity, with estimated depths of 6,060 m, 4,000 m, and 7,660 m, respectively.

Given the absence of seismic surveys, whose acquisition remains costly, we propose – towards evaluating and certifying the petroleum potential of the Upemba Rift – that future exploration work in these three prospective zones should be directed toward sedimentological studies, detailed mapping, and characterization of anomalous zones. This will allow precise identification of the most promising sites for future drilling within the Upemba Rift.

ACKNOWLEDGEMENTS

We express our profound gratitude to Mr. Elie Achille Manwana, whose provision of essential software greatly contributed to the preparation of the maps presented in this work. We also extend our sincere thanks to Mr. Djonive Munene Asidi for his guidance and advice, which enriched and directed our approach.

REFERENCES

- [1] Ministry of Hydrocarbons DRC, Atlas of Petroleum Blocks, Kinshasa/DRC, pp. 4-27, 2022.
- [2] Delvaux D., Fernandez-Alonso M., Petroleum potential of the Congo Basin, in de Wit M.J., Guillocheau F., de Wit M.C.J. (eds.), Geology and Resource Potential of the Congo Basin, Springer, Berlin/Germany, pp. 371-391, 2015.
- [3] Delhay F., Robert M., Contribution to the tectonic study of Katanga: relations between southern orogenic movements and major collapses in central Katanga, Annals of the Geological Society of Belgium, Liège/Belgium, pp. C5-C9, 1914.
- [4] De Magnée I., Geological cross-section of Mount Kibara (Katanga), Annals of the Geological Society of Belgium, Brussels/Belgium, pp. 201-206, 1935.
- [5] De Grand Ry G., African Grabens and petroleum exploration in East Africa, Royal Colonial Institute of Belgium, Brussels/Belgium, pp. 9-30, 1941.
- [6] Mortelmans G., Tectonic antecedents of the Upemba Graben, Bulletin Volcanologique, Paris/France, pp. 93-98, 1953.
- [7] Cahen L., Geology of the Belgian Congo, Vaillant-Caramanne, Liège/Belgium, 577p, 1954.
- [8] Aderca B.M., Geological note on Upemba National Park, Brussels/Belgium, pp. 1-2, 1961.
- [9] Compère P., Symoens J.J., The Zaire Basin, ORSTOM, Paris/France, pp. 401-456, 1987.
- [10] Kapajika B.C., Lecture notes on the geology of Africa and the Democratic Republic of Congo, UNIKOL, Lubumbashi/DRC, 51 p., 2013.
- [11] Muanza P.M., Presentation of geothermal potential and exploration status in the Democratic Republic of Congo, World Geothermal Congress, Melbourne/Australia, vol. 3, pp. 185-193, 2015.

- [12] Ngindu D., Tondozi K., Mukange A., Moshi F., Ikombi P., Mikobi W., New faults from the geodynamics of South Katanga in D.R. Congo, IJISRT, New Delhi/India, vol. 6/issue 1, pp. 1-10, 2021.
- [13] Ngindu D., Tondozi K., Mambu T., Upemba Rift and tectonics, Congolese Journal of Science and Technology, Kinshasa/DRC, vol. 2/issue 2, pp. 289-295, 2023.
- [14] Rumvegeri B.T., Tectonic importance of Kibarian structures in Central and East Africa, African Journal of Earth Sciences, Nairobi/Kenya, vol. 13/issue 2, pp. 267-276, 1991.
- [15] Robert M., Contribution to the morphology of Katanga: geographic cycles and peneplains, Royal Colonial Institute of Belgium, Brussels/Belgium, p. 49, 1939.
- [16] Tiercelin J.J., Lezzar K.E., A 300-million-year history of rift lakes in Central and East Africa: an updated broad review, in Odada E.O., Olago D.O. (eds.), The East African Great Lakes: Limnology, Paleolimnology and Biodiversity, Kluwer Academic Publishers, Dordrecht/Netherlands, pp. 3-60, 2002.
- [17] Diemu T.B., Petroleum potential of the Democratic Republic of Congo, University Press of Congo, Kinshasa/DRC, pp. 44-46, 2022.
- [18] CGG (Compagnie Générale de Géophysique), Technical report on geophysical methods applied to exploration, Paris/France, pp. 45-51, 1986.
- [19] Debeglia N., Geophysical methods applied to structural mapping, Review of Applied Geology, Paris/France, pp. 45-51, 2005.
- [20] El Gout M., Benali A., Rahmani S., Structural analysis of sedimentary basins using geophysical imaging, International Geoscience Meeting, Rabat/Morocco, vol. 3, pp. 185-193, 2009.
- [21] Fourier J., Analytical theory of heat propagation, Annals of Physics, Paris/France, vol. 1/issue 6, pp. 9-10, 1822.
- [22] Chen Z.X., Mou L., Meng X.H., The horizontal boundary and top depth estimates of buried sources using gravity data and their applications, Journal of Applied Geophysics, vol. 124, pp. 62-72, 2016.
- [23] Dubois P., Martin L., Koffi J., Geodynamic characterization of rift zones, Journal of Earth Sciences, Montreal/Canada, vol. 1/issue 6, pp. 9-10, 2011.
- [24] Cooper G.R.J., Euler deconvolution applied to potential field gradients, Exploration Geophysics, vol. 35, pp. 165-170, 2004.
- [25] Cella F., Fedi M., Florio G., Toward a full multiscale approach to interpret potential fields, Geophysical Prospecting, vol. 57, pp. 543-557, 2009.
- [26] Miller H.G., Singh V., Potential field tilt – a new concept for location of potential field sources, Journal of Applied Geophysics, vol. 32, pp. 213-217, 1994.
- [27] Verduzco B., Fairhead J.D., Green C.M., MacKenzie C., New insights into magnetic derivatives for structural mapping, The Leading Edge, vol. 23, pp. 116-119, 2004.
- [28] Salem A., Williams S., Fairhead J.D., Ravat D., Smith R., Tilt-depth method: A simple depth estimation method using first-order derivatives of potential fields, The Leading Edge, vol. 26, pp. 1502-1505, 2007.
- [29] Ferreira F.J.F., de Souza J., de Castro L.G., Edge detection in magnetic data using tilt derivatives, Geophysics, vol. 78, pp. J33-J41, 2013.

-
- [30] Cooper G.R.J., Cowan D.R., Enhancing potential field data using filters based on the local phase, *Computers & Geosciences*, vol. 32, pp. 1585-1591, 2006.
- [31] Thurstone L., Johnson M., Carter P., *Advances in Rift Basin Evolution*, International Geological Congress, Berlin/Germany, vol. 3, pp. 185-193, 1999.
- [32] Thurstone L., Carter P., Smith J., *Geodynamic Processes in Continental Rifting*, Earth Science Review, New York/USA, vol. 1/issue 6, pp. 9-10, 2002.
- [33] Tiercelin J.J., The tectonic rift that will split Africa in two: The East African Rift, *Science in the Present*, Encyclopedia Universalis, Paris/France, pp. 200-215, 2012.

Received: December 2025; Revised: February 2026; Accepted: February 2026; Published: February 2026